JOURNAL OF MATERIALS SCIENCE 27 (1992) 2067–2074

Theory and experiments on irregular eutectic growth: investigation on Al–Si eutectic growth

JUN-MIN LIU
National Laboratory of Solid State Microstructures, Nanjing University, Nanjing 210008, People's Republic of China

YAO-HE ZHOU, BAO-LU SHANG
Department of Materials Science and Engineering, Northwestern Polytechnical University, Xian 710072, People's Republic of China

Theoretical models of irregular eutectic growth are reviewed, and constrained growth of Al–Si eutectic has been experimentally investigated to quantitatively check these models. A thermal-difference amplifying method has been applied to measure the supercooling of the growing interface. Our results support a revised Jackson–Hunt model of interface supercooling. The dependence of the supercooling on temperature gradient is presented. At low growth rate, dependence of silicon branching on temperature gradient has been observed. The inter-phase spacing decreases with increases of growth rate and temperature gradient.

1. Introduction

In recent decades many studies of eutectic growth have been reported [1–8]. Significant progress in modelling regular eutectic growth has been made. However, much work remains to be done for the modelling of irregular eutectic growth, although a series of studies have also been made [9–13]. In this paper, theoretical models of irregular eutectic growth are briefly reviewed first. Our experimental investigation on the growth of irregular Al–Si eutectic under constrained conditions, aimed at obtaining a deep insight into the growth mechanisms of irregular eutectics and also checking the current models, is then presented.

2. Theoretical review

2.1. Supercooling of the growing interface

It is well known that the supercooling ΔT of the growing interface of a regular lamellar eutectic can be expressed as a function of the inter-phase spacing λ and growth rate V

$$\Delta T = K_1 \lambda V + \frac{K_2}{\lambda} \quad (1)$$

where K_1 and K_2 are two parameters which express the constitutional supercooling effect and the Gibbs–Thompson effect of the solid–liquid interface, respectively. In 1966, Jackson and Hunt [1] derived expressions for K_1 and K_2, based on the assumption of a planar isothermal growing interface as shown in Fig. 1a:

$$K_1 = \left(\frac{m_\alpha + m_\beta}{m_\alpha m_\beta}\right) \frac{P(1+\varepsilon)^2 C_0}{\varepsilon D_L \pi^3} \quad (2a)$$

$$K_2 = 2(1+\varepsilon)\left(\frac{\Gamma^\alpha \sin\theta_\alpha}{m_\alpha} + \frac{\Gamma^\beta \sin\theta_\beta}{\varepsilon m_\beta}\right) \quad (2b)$$

where m_α and m_β are the absolute values of the liquidus slopes of α and β phases, Γ^α and Γ^β are the Gibbs–Thompson coefficients of the α–liquid and β–liquid interfaces, respectively; θ_α, θ_β, S_α and S_β are denoted in Fig. 1a; C_0 is the difference between the maximum solubilities of two phases; D_L is the solute diffusion coefficient in liquid; $\varepsilon = S_\beta/S_\alpha$; P is the sum of a series:

$$P = \sum_{n=1}^{\infty} \frac{1}{n^3} \sin^2\left(\frac{n\pi}{1+\varepsilon}\right) \quad (2c)$$

The Jackson–Hunt model has been verified to be a good approach for the case of regular eutectic growth. However, the assumption of a planar growing interface neglects the coupling among the thermal transfer, the mass diffusion in liquid and the Gibbs–Thompson effect as well during growth. For the irregular eutectic case, in fact, the growing interface morphology is determined by this coupling, if the kinetic supercooling is omitted [14, 15]. This coupling results in a large dependence of λ as a function of the temperature gradient in liquid near to the growing interface, G_L, which has been shown by some experimental measurements [4, 9, 10, 14–19].

The curved solid–liquid interface and non-uniform interface wavelength (i.e. the spacing) λ are two important features of irregular eutectic growth. The typical interface morphology is schematically drawn in Fig. 1b. The amplitude of the interface along the growth direction is at least comparable to λ, or larger than λ. The argument that the interface is almost isothermal and planar seems to be incorrect for the case of an irregular eutectic.

0022–2461 © *1992 Chapman & Hall*

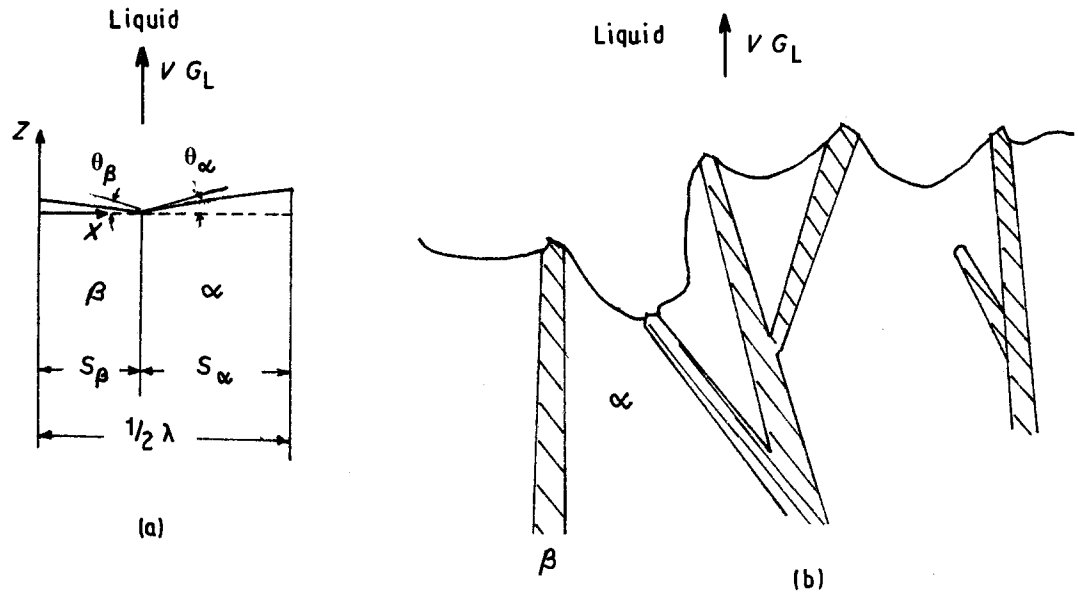

Figure 1 Sketches of the growing interface profile of regular eutectic (a) as proposed by Jackson and Hunt and (b) for an irregular eutectic. G_L is the temperature gradient.

Sato and Sayama [20] first considered this coupling. They noticed that for an irregular eutectic, commonly $S_\alpha \gg S_\beta$ (and/or one (β) of the two phases is faceted), so the middle range of the α–liquid interface will be concave into the solid side. They modelled the interface profile as drawn in Fig. 2a, and defined

$$\eta = w/S_\alpha \tag{3}$$

as the controlling parameter, then derived the following expressions for K_1 and K_2:

$$K_1 = \left(\frac{m_\alpha m_\beta}{m_\alpha + m_\beta}\right)\frac{C_0}{\pi D_L(1+\varepsilon)} \times\left[\left(1+\frac{\varepsilon}{\eta}\right)\ln\left(1+\frac{\eta}{2\varepsilon}\right) + \frac{\varepsilon}{4\eta}\ln\left(\frac{2\varepsilon}{\eta}+1\right)\right] \tag{4a}$$

$$K_2 = \frac{2m_\alpha m_\beta}{m_\alpha + m_\beta}(1+\varepsilon)\ln\left(\frac{2\varepsilon}{\eta}+1\right) \times\left(\frac{\Gamma^\alpha \varepsilon \sin\theta_\alpha}{\eta m_\alpha} + \frac{\Gamma^\beta \sin\theta_\beta}{m_\beta}\right) \tag{4b}$$

The Sato–Sayama model does not tell us how to calculate the parameter η. Moreover, the interface morphology observed experimentally differs from that shown in Fig. 2a. The coupling relation can be written as

$$\Delta T = \Delta T^* - G_L Z \tag{5}$$

where ΔT^* is the supercooling at the three-phase conjunction point ($X = S_\beta$, $Z = 0$). This coupling relation is no doubt reasonable. However, as we have pointed out above, the morphology of the growing interface should be completely determined by the coupling relation and the corresponding boundary conditions, so an arbitrary controlling parameter (η) is unnecessary to calculate the interface profile. Nash [21] has derived a differential–integral equation to describe this coupling. In order to solve this equation, Nash also used the assumption of a planar isothermal growing interface to simplify numerical calculation. Therefore, Nash's solution may not be applied to the case of irregular eutectic growth as well. Fisher and Kurz [22] argued that the growing interface profile can be expressed by a polynomial, which satisfies the boundary conditions. They derived this polynomial as

$$\frac{Z^*(X)}{S_\alpha} = \tan\theta_\alpha\left[(2\varphi+1)\left(\frac{X-S_\beta}{S_\alpha}\right)^3 - (3\varphi+2)\left(\frac{X-S_\beta}{S_\alpha}\right)^2 - \left(\frac{X-S_\beta}{S_\alpha}\right)\right] \tag{6}$$

where $Z^*(X)$ denotes the interface profile, $\varphi = 2\varepsilon(1+\varepsilon)/(\lambda\varepsilon + g\theta_\alpha)$, $w = S_\beta + f_1 S_\alpha$, $g = \tan\theta_\alpha \times[(6\varphi+3)f_1^2 - (6\varphi+4)f_1 + 1]$, $f_1 = [(2+3\varphi) - (9\varphi^2+4\varphi)^{1/2}]/(2+4\varphi)$; δ and w are defined in Fig. 2b. Expressions for K_1 and K_2 are written as

$$K_1 = \left(\frac{m_\alpha m_\beta}{m_\alpha + m_\beta}\right)\frac{C_0(1+\varepsilon)}{\pi^3 D_L}\left(P + \frac{\Pi}{f_1\varepsilon}\right) \tag{7a}$$

$$K_2 = \frac{2(1+\varepsilon)}{m_\alpha + m_\beta} \times\left(m_\alpha \Gamma^\alpha \sin\theta_\beta + \frac{m_\beta \Gamma^\alpha \sin\theta_\alpha - \sin(\tan^{-1} g)}{f_1\varepsilon}\right) \tag{7b}$$

where

$$\Pi = \sum_{n=1}^{\infty}\left(\frac{\sin[n\pi(1+\varepsilon)]\sin[(1+f_1\varepsilon)/(1+\varepsilon)]}{n^3}\right) - P$$

Fisher and Kurz [22] used the following approximative coupling equation to determine the factor δ:

$$\Delta T|_{0 \le X \le S_\beta} = \Delta T|_{S_\beta < X \le (S_\beta + w)} = \Delta T|_{(S_\beta + w) < X \le (S_\alpha + S_\beta)} + G_L\delta \tag{8}$$

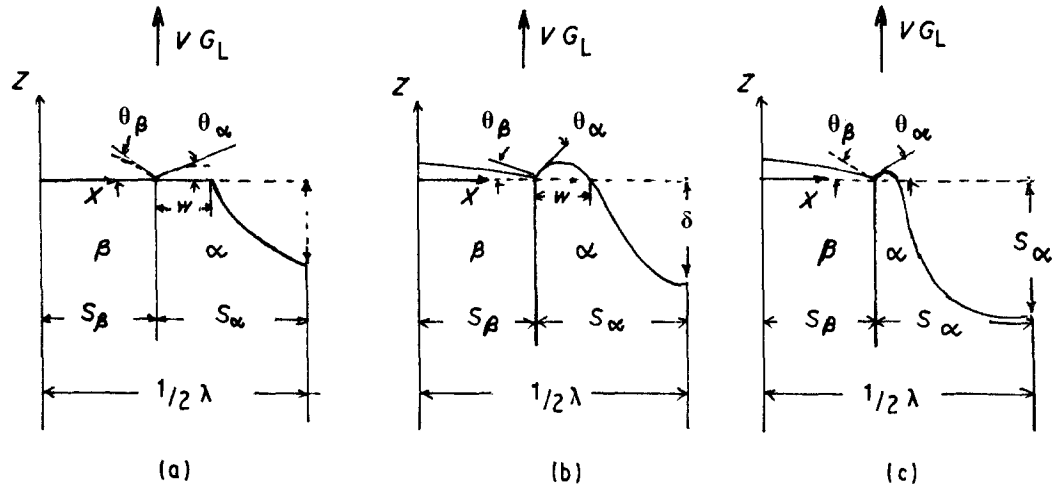

Figure 2 Sketches of the growing interface profile of irregular eutectic, proposed by (a) the Sato–Sayama model, (b) the Fisher–Kurz model and (c) the revised Jackson–Hunt model.

They declared that ΔT and the interface profile can be calculated with Equation 8.

For the case of an irregular eutectic, under common conditions of growth λ is of the order of micrometres, so the Gibbs–Thompson effect is very weak. The primary contribution to ΔT comes from the constitutional supercooling. In earlier work [23] we have modelled the α–liquid interface profile as a semicircle (in three dimensions, it is a semi-cylindrical surface), as drawn in Fig. 2c, and derived the following expressions for K_1 and K_2:

$$K_1 = \frac{m_\alpha + m_\beta}{m_\alpha m_\beta}\left(\frac{P(1+\varepsilon)^2 C_0}{\varepsilon D_L \pi^3} + \frac{C_E - C_{\alpha m}}{\pi D_L (1+\varepsilon)}\right) \quad (9a)$$

$$K_2 = 2(1+\varepsilon)\Gamma^\alpha \sin\theta_\alpha \left(\frac{m_\beta}{m_\alpha + m_\beta}\right) \quad (9b)$$

where $C_{\alpha m}$ is the maximum solubility of the α phase at the equilibrium temperature. We name Equation 9 the revised Jackson–Hunt model.

Pandley and Ramachandrarao [24] also recently set up a coupling relation satisfied by lamellar eutectic growth, although the expressions for K_1 and K_2 were not directly given. This relation can be rewritten as

$$1 - \frac{\tanh(P_\alpha S_\alpha)}{P_\alpha S_\alpha} = \varepsilon \frac{C_0^\beta}{C_0^\alpha}\left(\frac{m_\alpha C_0^\alpha + (G_L D_L/V)}{m_\beta C_0^\alpha + (G_L D_L/V)}\right) \times \left(1 - \frac{\tanh(P_\beta \varepsilon S_\alpha)}{P_\beta \varepsilon S_\alpha}\right) \quad (10)$$

where $P_\alpha^2 = (m_\alpha A_\alpha + G_L)/\Gamma^\alpha$, $P_\beta^2 = (m_\beta A_\beta + G_L)/\Gamma^\beta$, $A_\alpha = VC_0^\alpha/D_L$, $A_\beta = VC_0^\beta/D_L$, $C_0^\alpha = C_E - C_{\alpha m}$, $C_0^\beta = C_{\beta m} - C_E$; $C_{\beta m}$ and C_E are the maximum solubility of β phase and the eutectic concentration at the equilibrium temperature, respectively. Equation 10 differs in form from Equation 1. For the Al–Si eutectic, we have made calculation and obtained a similar form to Equation 1 from the Pandley model [24]:

$$\Delta T = (-1.82 \times 10^{-7})\lambda V + \frac{0.139}{\lambda} \quad (\mu m, s, K) \quad (11)$$

where $K_1 < 0$ is apparently unreasonable. Hence the Pandley model [24] seems also not to be a good approach for the case of an irregular eutectic.

2.2. Selection of the spacing λ

Selection mechanisms of the spacing λ, at least for an irregular eutectic, have not so far been understood. Jackson and Hunt [1] used the extremum condition proposed by Zener (see also [1]), which yielded the following scaling relation of λ and V from Equation 1:

$$\lambda^2 V = K_2/K_1 \quad \lambda = \lambda_e \quad (12)$$

For irregular eutectic growth, the selection of λ measured by experiments, λ_S, is much larger than λ_e. Similar scaling relations are suggested by the Sato–Sayama model [20] and the Fisher–Kurz model [22]. For the Al–Si eutectic, Fisher and Kurz obtained

$$\lambda^2 V = (8.01 \times 10^4) G_L^{-0.81} \quad (\lambda:\mu m,\ V:\mu m\ s^{-1},\ G_L:K\ cm^{-1}) \quad (13)$$

Equation 13 gives λ as a function of both V and G_L. Pandley and Ramachandrarao [24] declared that λ should satisfy Equation 10. In fact, we can rewrite Equation 10 to give

$$\frac{P_\alpha S_\alpha - \tanh(P_\alpha S_\alpha)}{P_\beta S_\beta - \tanh(P_\beta S_\beta)} = f(\lambda) = \frac{P_\alpha C_0^\beta}{P_\beta C_0^\alpha}\left(\frac{m_\alpha C_0^\alpha + (G_L D_L/V)}{m_\beta C_0^\alpha + (G_L D_L/V)}\right) = K \quad (14)$$

Unfortunately, we find that $f(\lambda)$ oscillates irregularly with λ for the case of the Al–Si eutectic. No unique selection of λ can be obtained from Equation 14.

We have briefly reviewed and discussed some current models for irregular eutectic growth. In addition, some experimental reports have also been published [16–19]. It has been shown that there are two large obstacles: the first is that measurement of ΔT is technically very difficult; the second is that the holding of a constant temperature gradient during growth is not easy. So far, quantitative checking of these models has

not been done because of a lack of enough experimental data. Therefore, further experiments on irregular eutectic growth are required. In this paper, we will present our preliminary experimental results on Al–Si eutectic growth under constrained conditions.

3. Experimental procedure

In our experiments the supercooling ΔT of the growing interface and the inter-phase spacing λ were treated as functions of V and G_L. The experiments were done on a unidirectional solidification apparatus. The samples were prepared by melting high-purity aluminium and single crystals of silicon in vacuum induction furnace and casting into cylindrical bars of $\phi 8 \times 140$ mm. Each sample was set into a high-purity graphite tube. The tube was put vertically into an alumina pipe surrounded by two heaters. The sample was heated to 1000 °C and held for 30 min. The graphite tube was then lowered into a freezer connected with the bottom of the alumina pipe. The cooling medium in the freezer was liquid Ga–In–Sn alloy with a freezing point of 5 °C. The freezer and the alumina pipe moved upward relative to the sample at a constant speed V_P. Because the freezer could effectively cool the end part of the sample, the temperature distribution in the liquid zone ahead of the solid–liquid interface remained linear and unchanged; G_L was then constant during growth. Each sample grew for 6–8 cm and was then quenched into water at room temperature. Since λ was ~ 10 μm, the steady state of growth was considered to be reached after an initial growth of 10 mm.

In our experiments a thermal-difference amplifying method was applied to measure ΔT. The principle of this method is shown in Fig. 3a. Two pairs of NiCr–NiSi thermocouples are fixed in the liquid zone about 30–40 mm above the initial solid–liquid interface, with a 1 mm vertical distance between their joints (a) and (b). While the growing interface moves upward and contacts with joint (a), latent heat released from the interface will heat the micro-zone around (a). About 0.02 °C elevation in this zone leads to a small change of thermal-potential difference between (a) and (b), which is amplified by an amplifier into a signal of the order of millivolts and recorded by an X–Y recorder. The recorder records meanwhile the thermal-potential change of joint (a) with time. Typical recorded curves are shown in Fig. 3b, where curve F is the variation of the potential difference between (a) and (b) with time; the valley in F indicates that the growing interface is arriving at joint (a). Curve E indicates the change of temperature at joint (a) with time. That point on curve E which corresponds to the valley of curve F is the temperature of the growing interface T_M; $\Delta T = T_e - T_M$, where T_e is the equilibrium temperature. We can also easily obtain the value of G_L with the aid of curve E and the growth rate measured by a dial gauge.

Our measurements show that effective cooling of the freezer can guarantee synchronization of the moving speed V_P of the freezer and the growth rate V of the sample, provided $V \leq 120\ \mu m\,s^{-1}$. Even if $V > 120\ \mu m\,s^{-1}$, the movement of the solid–liquid interface relative to the freezer is also very small. Therefore V is taken to be equal to V_P.

The solidified samples were cut longitudinally and radially. The inter-phase spacing λ was measured on longitudinal sections of the samples by a micrometer in a microscope. The solidified structures are for example shown in Fig. 4, where the line crosses a number of silicon flakes. The ratio of the length of

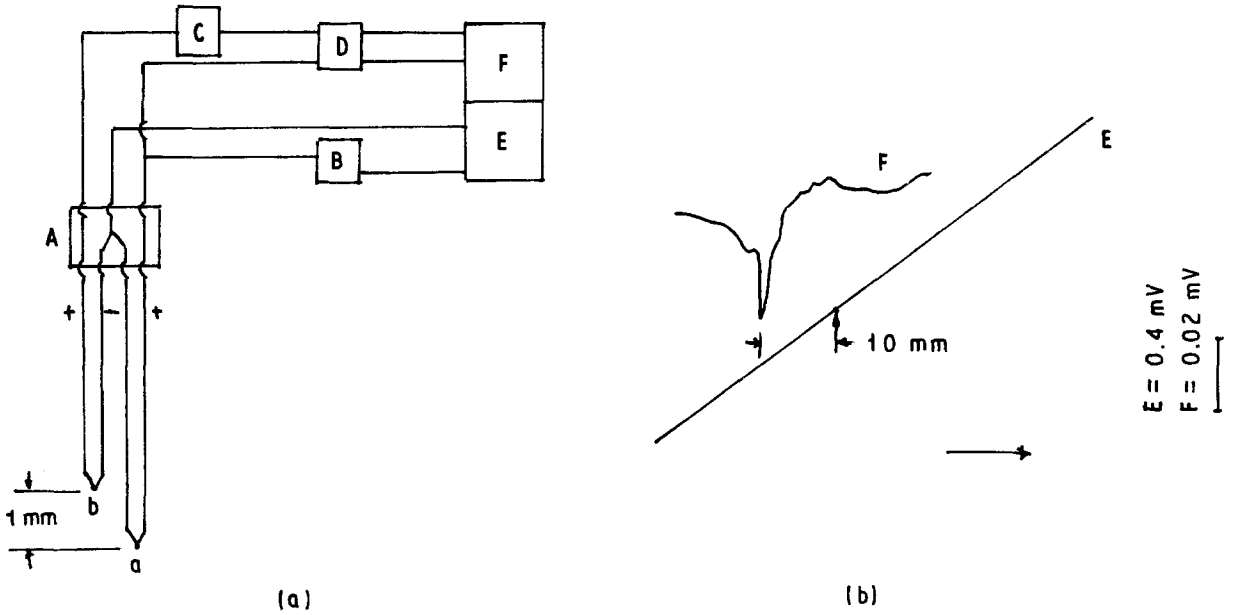

Figure 3 Measurement of the supercooling ΔT of the growing solid–liquid interface by the thermal-difference amplifying method. (a) Principle of the method: a, b two pairs of NiCr–NiSi thermocouples, (A) box filled with mixed ice and water, (B, C) zero-potential-set units, (D) amplifier, (E, F) recorders. (b) Curves recorded by recorders E and F (paper speed 30 mm min^{-1}). T_e is the equilibrium temperature at the eutectic point; $\Delta T = T_e - T$.

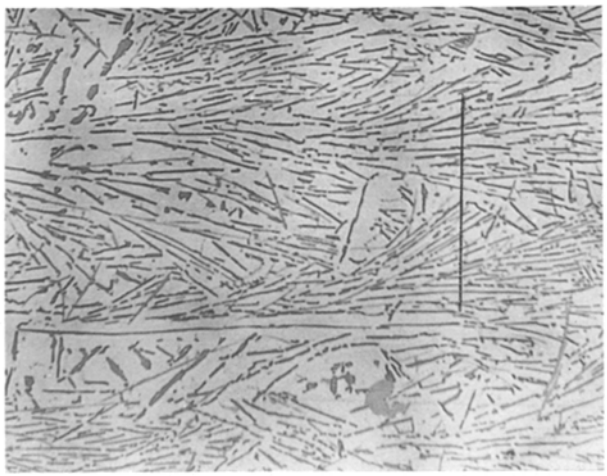

Figure 4 Solidified microstructure of Al–Si eutectic under constrained conditions: longitudinal section, growth direction from left to right, magnification ×160. $V = 9.66\ \mu m\ s^{-1}$, $G_L = 149\ K\ cm^{-1}$.

the line to the number of the flakes equals λ. 20 regions of each sample were measured, and the average of measured values λ_S, was denoted by λ_m.

It has been noticed that the growth laws are different for different ranges of growth conditions. In our discussion the following four ranges will be dealt with:

$$\text{A: } 0.63\ \mu m\ s^{-1} \leq V \leq 40.00\ \mu m\ s^{-1}$$
$$8\ K\ cm^{-1} \leq G_L \leq 77\ K\ cm^{-1}$$
$$\text{B: } 0.63\ \mu m\ s^{-1} \leq V \leq 40.00\ \mu m\ s^{-1}$$
$$78\ K\ cm^{-1} \leq G_L \leq 149\ K\ cm^{-1}$$
$$\text{C: } 19.50\ \mu m\ s^{-1} \leq V \leq 206\ \mu m\ s^{-1}$$
$$8\ K\ cm^{-1} \leq G_L \leq 77\ K\ cm^{-1}$$
$$\text{D: } 19.50\ \mu m\ s^{-1} \leq V \leq 206\ \mu m\ s^{-1}$$
$$78\ K\ cm^{-1} \leq G_L \leq 149\ K\ cm^{-1}$$

where A and B are ranges with low growth rate, while C and D are ranges with high growth rate.

4. Results and comparisons

4.1. Supercooling ΔT

4.1.1. Comparison

Experimental results are listed in Table I. We have also used the experimental data obtained by Hogan and Song [19] and Elliott and Glenister [17] in order to pile up as many data as possible. Table II shows some physical parameters of the Al–Si eutectic [5]. We have calculated the values of parameters K_1 and K_2 according to the models described in section 2. The results calculated and regressed from experiments are listed in Table III.

We can conclude from Table III the following: among these models, only the Jackson–Hunt model and the revised Jackson–Hunt one are close to the experimental data. In detail, consistency of the Jackson–Hunt model with the data of ranges C and D can be seen, and differences between the revised Jackson–Hunt model and the data of all four ranges are small.

TABLE I Parts of the experimental data for steady-state growth of Al–Si eutectic under constrained conditions

Sample	V ($\mu m\ s^{-1}$)	G_L ($K\ cm^{-1}$)	λ (μm)	ΔT (K)
01	0.63	77.55	28.03 ± 1.72	0.25
02	1.04	149.00	28.57 ± 1.80	0.42
03	1.75	77.55	27.58 ± 1.66	0.68
04	5.05	100.50	13.71 ± 2.51	0.86
05	5.10	90.90	13.33 ± 2.54	0.96
06	5.18	149.00	9.66 ± 0.90	0.86
07	5.43	42.53	13.62 ± 0.92	1.34
08	9.66	149.00	8.02 ± 0.32	1.46
09	9.71	63.00	9.34 ± 2.17	2.22
10	9.84	149.00	7.95 ± 1.47	1.74
11	9.95	129.40	8.41 ± 1.23	2.17
12	11.36	42.51	9.54 ± 1.41	2.14
13	19.50	106.00	6.23 ± 0.85	1.84
14	20.12	95.95	6.60 ± 0.74	2.74
15	20.45	42.53	8.21 ± 1.92	2.92
16	20.50	149.00	5.61 ± 0.39	2.26
17	25.32	95.00	6.24 ± 0.70	2.28
18	38.47	102.80	5.51 ± 0.44	3.29
19	40.00	101.00	5.47 ± 0.41	3.35
20	70.00	95.95	4.00 ± 0.59	3.89
21	74.90	106.80	4.03 ± 0.06	3.56
22	121.00	77.10	3.46 ± 0.20	7.11
23	206.00	69.43	2.98 ± 0.17	8.42

TABLE II Physical parameters of Al–Si eutectic [5]

Parameter	Value
C_0	98.35 wt %
$C_{\alpha m}$	1.56 wt %
m_β	20 K (wt %)$^{-1}$
P	0.34882
Γ^β	0.125 K μm
$\theta_\alpha, \theta_\beta$	30°
$C_{\beta m}$	100.00 wt %
D_L	$5 \times 10^3\ \mu m^2\ s^{-1}$
m_α	8.3 K (wt %)$^{-1}$
ε	5.993
Γ^α	0.106 K μm
C_E	12.62 wt %

TABLE III Comparison between models and experiments for the parameters K_1 and K_2 for Al–Si eutectic growing under constrained conditions

	K_1 ($K\ s\ \mu m^{-2}$)	K_2 ($K\ \mu m^{-1}$)
Theory		
Jackson–Hunt	9.61×10^{-3}	0.567
Sato–Sayama	8.49×10^{-5}	1.449
Fisher–Kurz	-4.30×10^{-4}	1.348
Pandley	-1.82×10^{-7}	0.139
Revised Jackson–Hunt	14.10×10^{-3}	0.090
Experiment		
Range A	16.71×10^{-3}	2.541
Range B	17.41×10^{-3}	2.284
Range C	10.87×10^{-3}	−3.056
Range D	10.16×10^{-3}	1.861
Range C + D	11.66×10^{-3}	−0.763

On the other hand, the contribution of the constitutional supercooling to ΔT is always dominant, and the Gibbs–Thompson effect is weak. The comparison between the models and the measured data for ΔT as

a function of the term λV for ranges C + D and A + B are shown in Fig. 5a and b, respectively. In the C + D range, linear dependence of ΔT as a function of the term λV is presented. In the A + B range, the measured curve of ΔT as a function of λV is slowly concave upward, which means that the Gibbs–Thompson effect becomes relatively more important. Generally speaking, of these models the revised Jackson–Hunt model of ΔT obtains the strongest support from the measured data. In fact, the most important feature of irregular eutectic growth is the deep concavity into the solid side of the middle range of the α–liquid interface. There is strong pile-up of solute within the concave zone. The revised Jackson–Hunt model has considered this feature, although some unimportant points are neglected.

4.1.2. Influence of temperature gradient

So far, no quantitative expression for ΔT as a function of G_L has been given. Our experiments show that ΔT decreases with increasing G_L, as shown in Fig. 6. In our opinion, an increase of G_L makes the interface profile closer to planar, and solute pile-up within the concave zone is decreased. The Gibbs–Thompson effect is also weakened because the curvature of the growing interface is reduced. Therefore, both K_1 and K_2 in Equation 1 will be lowered.

When V is held unchanged, ΔT as a function of G_L can be determined by Equation 5. Therefore, the dependence of ΔT on G_L is at least in part considered by models other than the Jackson–Hunt one.

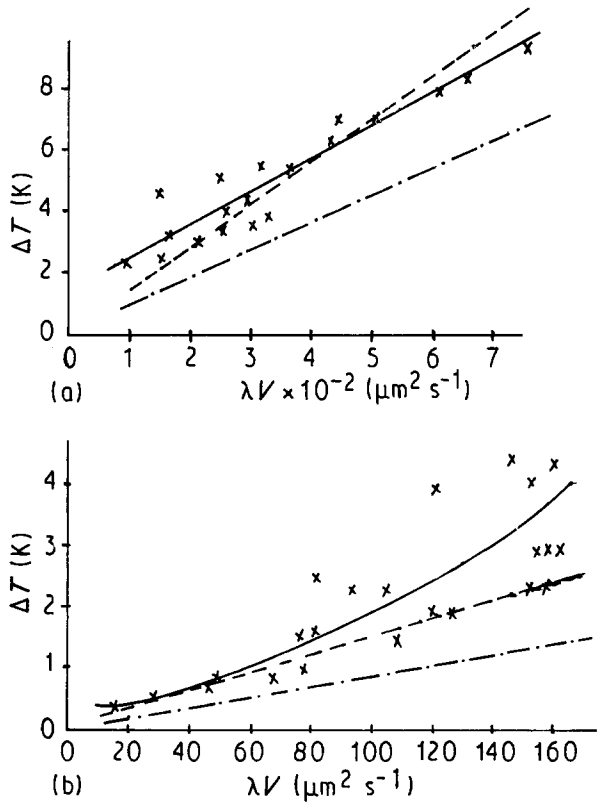

Figure 5 Comparisons between models and experiments for the interface supercooling ΔT as a function of the term λV for Al–Si eutectic growth under constrained conditions. (a) Growth in range (C + D), (×) experimental results, (–·–) Jackson–Hunt model, (– – –) revised Jackson–Hunt model. (b) Growth in range (A + B).

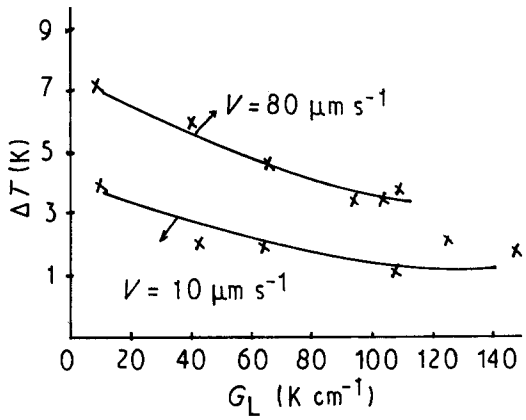

Figure 6 Interface supercooling ΔT as a function of G_L for Al–Si eutectic growing under constrained conditions.

4.2. Selection of the spacing

The spacing λ as a function of V and G_L is regressed according to the formula

$$\lambda^m V = K_3 G_L^{-n} \quad m > 0,\ n > 0 \qquad (15)$$

The regressed results are listed in Table IV. Unfortunately, none of the models is supported by the experimental results. Equation 13 obtained by Fisher and Kurz [22] is close to the regressed equation for the C + D range, but quantitative consistence has not been shown. These comparisons show that our insight into the selection mechanisms of the spacing for irregular eutectic growth under steady-state conditions is very limited. However, we will analyse the experimental data in more detail.

Except in range A (low V and low G_L), the spacing λ as a function of G_L decreases with increase of G_L. In range D, dependence of λ on G_L is comparable to that of λ on V. In range A, we have

$$\lambda \cong K_3 V^{-0.34} \qquad K_3 > 0, \text{ constant} \qquad (16)$$

i.e. λ is only determined by V. Another characteristic shown in Table IV is that only in range D, the exponent $m \cong 2$. In other ranges, $m > 2$ (m is close to 3 in range A) which cannot be reasonably explained by the current models.

For irregular eutectic growth, since the difference in volume fraction of the two phases is large, moreover, the phase of smaller volume fraction (β phase) is commonly faceted; the growing interface is curved in morphology and non-isothermal. If the interface deviates from a plane in morphology, m will not equal 2. For the Al–Si eutectic, $m > 2$ since the middle part of the α–liquid interface is largely concave into the solid side [14, 15]. The current models, except the Jackson–Hunt one, have taken this deviation into account, and introduced G_L into parameters K_1 and K_2, which hence become functions of G_L. However, in these models the extremum condition proposed by Zener [1] is still used to derive the expression for λ as a function of V and G_L, so $m \equiv 2.0$. Naturally, in the range D of high V and G_L, the growing interface is constrained to become closer to the planar, then m tends to 2.

During irregular eutectic growth, the faceted β phase commonly branches continuously because of

TABLE IV Experimental results for growth of Al–Si eutectic under constrained conditions (r = correlation coefficient)

Range	V ($\mu m\,s^{-1}$)	G_L ($K\,cm^{-1}$)	$\lambda^m V = K G_L^{-n}$	r
A	0.63–40.00	8–77	$\lambda^{2.87} V = (1.27 \times 10^4) G_L^{0.02}$	0.97
B		96–149	$\lambda^{2.18} V = (4.37 \times 10^3) G_L^{-0.31}$	0.96
A + B		8–149	$\lambda^{2.11} V = (5.43 \times 10^3) G_L^{-0.38}$	0.97
C	19.5–206.0	8–77	$\lambda^{2.67} V = (3.19 \times 10^4) G_L^{-0.49}$	0.99
D		96–149	$\lambda^{2.01} V = (3.22 \times 10^5) G_L^{-1.25}$	0.97
C + D		8–149	$\lambda^{2.09} V = (7.20 \times 10^3) G_L^{-0.39}$	0.95

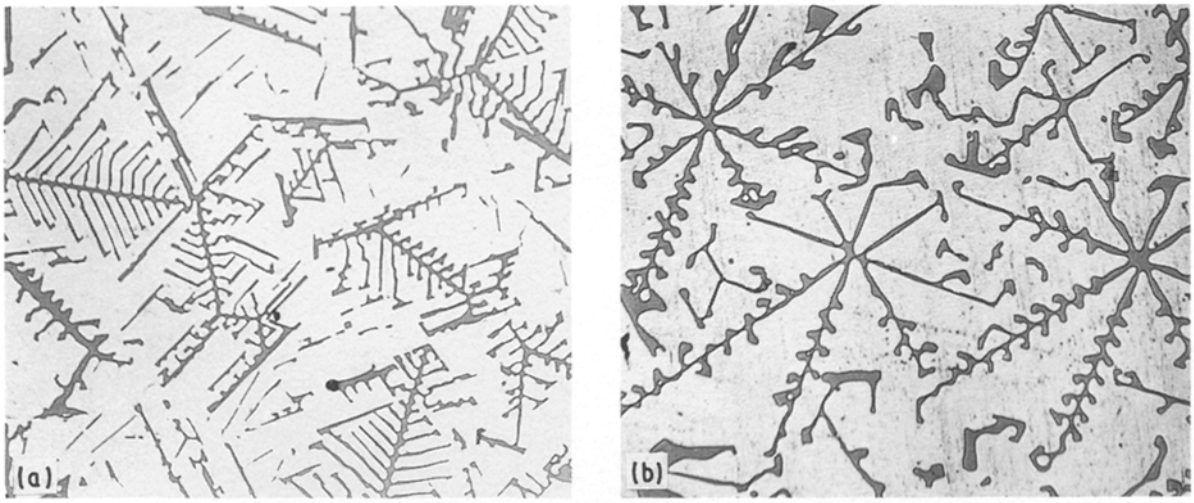

Figure 7 Photographs showing the dependence of the branching number of silicon flakes on G_L for Al–Si eutectic growing under constrained conditions; $V \cong 0.94\ \mu m\,s^{-1}$, radial sections, magnification $\times 200$. (a) $G_L = 149\ K\,cm^{-1}$, (b) $G_L = 77\ K\,cm^{-1}$.

its strong crystalline anisotropy. High growth rate (or high temperature gradient) constrains branching of the faceted phase, but the branching can also fully develop at low growth rate or temperature gradient. For the Al–Si eutectic at low V, strong dependence of the number of primary branches of silicon flakes on G_L has been observed. Fig. 7 shows variation of the number of silicon branches from 8 to 5 as G_L varies from 77 to 149 $K\,cm^{-1}$. This effect will no doubt result in λ being an increasing function of G_L. On the other hand, λ should be lowered with increasing G_L, because ΔT as an approximative linearly increasing function of λ (as V is held constant, as shown in Fig. 5) is lowered as G_L increases. Therefore, at low V and G_L, λ is nearly independent of G_L, as shown in Equation 16. At high V, the exponent n in Equation 15 will become positive and increase with V, since the number of silicon branches shows a weak dependence on G_L.

5. Conclusions

Experimental data for interface supercooling seem to support a revised Jackson–Hunt model. The interface supercooling is contributed mainly by the constitutional supercooling effect. Therefore, the interface supercooling is an approximately linear function of the term λV. The interface profile as a function of temperature gradient G_L is constrained to become closer to the planar as G_L increases, and hence the interface supercooling as a function of G_L decreases with G_L.

Our experiments show that at low growth rate, the number of primary branches of silicon flakes decreases with increasing G_L. For different ranges of growth conditions, the spacing λ, as a function of G_L and growth rate V, has different expressions. When both G_L and V are low, the spacing depends only on V. In other ranges of growth conditions the spacing is decreased with increasing V or G_L. None of the current models is supported by our experiments on the selection of the spacing λ.

References

1. K. A. JACKSON and J. D. HUNT, *Trans. Metall. AIME* **236** (1966) 1129.
2. R. M. JORDAN and J. D. HUNT, *Metall. Trans.* **3** (1972) 1385.
3. M. N. CROKER, R. S. FIDLER and R. W. SMITH, *Proc. R. Soc.* **A335** (1973) 15.
4. R. ELLIOTT, "Eutectic Solidification Processings" (Butterworths, London, 1983) p. 120.
5. W. KURZ and D. J. FISHER, "Fundamentals of Solidification" (Trans. Tech., Aedermannsdorf, 1984) p. 202.
6. S. CHANDRASEKHAR, G. F. EISA and W. R. WILCOX, *J. Cryst. Growth* **76** (1986) 485.
7. R. TRIVEDI, P. MAGNIN and W. KURZ, *Acta Metall* **35** (1987) 971.
8. A. KARMA, *Phys. Rev. Lett.* **59** (1987) 71.
9. R. ELLIOTT, *Int. Met. Rev.* (1977) 161.

10. W. KURZ and D. J. FISHER, *ibid.* (1979) 177.
11. M. A. SAVAS and R. W. SMITH, *J. Mater. Sci.* **20** (1985) 881.
12. R. S. FIDLER, M. N. CROKER and R. W. SMITH, *J. Cryst. Growth* **13/14** (1972) 739.
13. M. N. CROKER, M. McPARLAN, D. BARAGAR and R. W. SMITH, *ibid.* **29** (1975) 85.
14. J.-M. LIU, Y.-H. ZHOU and B.-L. SHANG, *Acta Metall.* **38** (1990) 1625.
15. *Idem, ibid.* **38** (1990) 1631.
16. B. TOLOUI and A. HELLAWELL, *ibid.* **24** (1976) 565.
17. R. ELLIOTT and S. M. D. GLENISTER, *ibid.* **28** (1980) 1489.
18. S. M. D. GLENISTER and R. ELLIOTT, *Met. Sci.* **15** (1981) 181.
19. L. M. HOGAN and H. SONG, *Metall. Trans.* **18A** (1987) 707.
20. T. SATO and Y. SAYAMA, *J. Cryst. Growth* **22** (1974) 259.
21. G. E. NASH, *ibid.* **38** (1977) 55.
22. D. J. FISHER and W. KURZ, *Acta Metall.* **28** (1980) 777.
23. J.-M. LIU, Y.-H. ZHOU and B.-L. SHANG, *Met. Sci. Tech. Sinica* **8(2)** (1989) 34 (in Chinese).
24. L. PANDLEY and P. RAMACHANDRARAO, *Acta Metall.* **35** (1987) 2549.

Received 22 November 1990
and accepted 2 August 1991